Relaxometry for detecting free radical generation during Bacteria's response to antibiotics

Norouzi, Neda; Nusantara, Anggrek Citra; Ong, Yori; Hamoh, Thamir; Nie, Linyan; Morita, Aryan; Zhang, Yue; Mzyk, Aldona; Schirhagl, Romana

Published in:
Carbon

DOI:
10.1016/j.carbon.2022.08.025

Publication date:
2022

Carbon 199 (2022) 444–452

Contents lists available at ScienceDirect

Carbon

journal homepage: www.elsevier.com/locate/carbon

Relaxometry for detecting free radical generation during Bacteria's response to antibiotics

Neda Norouzi [a], Anggrek Citra Nusantara [a], Yori Ong [a], Thamir Hamoh [a], Linyan Nie [a], Aryan Morita [a,b], Yue Zhang [a], Aldona Mzyk [a,c], Romana Schirhagl [a,*]

[a] Groningen University, University Medical Center Groningen, Antonius Deusinglaan 1, 9713 AV Groningen, the Netherlands
[b] Dept. Dental Biomedical Sciences, Faculty of Dentistry, Universitas Gadjah Mada, Jalan Denta 1 Sekip Utara, Yogyakarta, 55281, Indonesia
[c] Institute of Metallurgy and Materials Science, Polish Academy of Sciences, Reymonta 25, 30-059, Krakow, Poland

ARTICLE INFO

Keywords:
Diamond relaxometry
Free radical
Bacterial response
Antibiotics

ABSTRACT

Free radical generation plays a key role in killing bacteria by antibiotics. However, radicals are short-lived and reactive, and thus difficult to detect for the state of the art. Here we use a technique which allows optical nanoscale magnetic resonance imaging (MRI) to detect radical generation on the scale of single bacteria. We demonstrate that the radical generation in *Staphylococcus aureus* increases in the presence of UV irradiation as well as vancomycin and is dependent on the antibiotic's dose. With a method based on ensembles of nitrogen vacancy (NV) centers in diamond, we were able to follow the radical formation near individual bacteria over the whole duration of the experiment to reveal the dynamics of radical generation. Using this new approach, we observed free radical concentrations within nanoscale voxels around the diamond particles and determined its exact timing depending on the antibiotic dose. Since changes in the response to antibiotics emerge in only a few bacteria of the entire population, such a single-cell approach can prove highly valuable for research into drug resistance.

1. Introduction

One of the most remarkable properties of fluorescent nanodiamonds (FNDs) is that they can be used for sensing magnetic fields by diamond magnetometry. This method is based on a paramagnetic defect in diamond, the so-called nitrogen vacancy (NV) center, which can be used as a sensor for its magnetic surrounding. The NV centers' fluorescence emission is brighter when excited from its $|m_s = 0>$ magnetic state compared to its $|m_s = \pm 1>$ state. Since the populations of these states are affected by the NV center's magnetic surrounding, one can read out a local magnetic resonance by measuring the fluorescence of the defect. This new technique has already been successfully used in physics to measure magnetic vortices [1], fields caused by nanostructures [2] or molecules on the diamond surface [3–5].

Apart from their optical properties, these FNDs also have excellent biocompatibility which has been demonstrated for many different cell types and for entire organisms [6–9]. This enables their use as sensors for spin noise produced by biological free radicals. To achieve this goal, we make use of a specific mode of diamond magnetometry called relaxometry [10–12]. During a relaxometry measurement, the NV centers are polarized into the bright $|m_s = 0>$ state of the ground state by a laser pulse. We then observe the fluorescence intensity after different dark times to evaluate the rate at which the NV center returns to the dark equilibrium between $|m_s = \pm 1>$ and $|m_s = 0>$. With this method it is possible to measure free radical formation in living yeast cells and radical production from mitochondria, since the spin noise accelerates the return to the dark equilibrium state [13,14].

Here we applied this method to detect paramagnetic compounds released in the process of bactericidal antibiotics killing bacteria. A prerequisite for such measurements is the biocompatibility of FNDs with bacteria. Indeed, FNDs show good biocompatibility with *Staphylococcus aureus*, the bacterium researched in this work [15,16]. While smaller detonation nanodiamond particles may be used with or without surface modification as antibacterial agents [17–19], recent observations showed that FNDs are not antibacterial but might induce aggregation in a *staphylococcal* Extracellular Polymeric Substance (EPS) producing strain (*S. aureus ATCC 12600*) [16]. In earlier work, Le Sage et al. have reported magnetometry of the magnetosomes of magnetotactic bacteria

* Corresponding author.
E-mail address: romana.schirhagl@gmail.com (R. Schirhagl).

https://doi.org/10.1016/j.carbon.2022.08.025
Received 12 April 2022; Received in revised form 15 July 2022; Accepted 3 August 2022
Available online 10 August 2022

[2]. However, their method detects static magnetic fields rather than spin noise from radicals.

Bacteria and how they are killed by antibiotics were investigated in this work for various reasons outlined in the following. According to a statistic by the American National Institute of Health (NIH) [20] between 5 and 10% of all hospitalized patients develop a bacterial infection. About 90,000 of these patients die each year as a result of their infection, compared to 13,300 patient deaths in 1992. A large part of this increase is attributed to an increase in antibiotic resistance. Technologies that allow for detailed monitoring of drug-cell interactions will greatly benefit our understanding and ability to control this problem in the long run.

In the context of antibiotic resistance, we are particularly interested in free radical formation since it plays a key role in the response to antibiotics [21–24]. There are even some indications that free radical formation might be a unifying factor that all killing mechanisms for all classes of antibiotics have in common [25,26]. Kohanski et al. demonstrated that all bacteria produce free radicals in response to all bactericidal drug classes while bacteriostatic drugs do not have this ability [25]. However, this is a topic of debate in the community [27]. Despite their relevance, relatively little is known about how free radicals work, where they are generated, and which ones exactly play a role. Due to their reactivity, they are difficult to distinguish from each other by specific assays. Quantifying, identifying and localizing them has been identified as the main bottleneck to understand their working mechanisms and as a consequence, translate free radical biology into medical advances [28].

In this work, we investigated the effect of vancomycin, which belongs to a group of bactericidal antibiotics that is widely used, specifically for autolysis of Gram-positive bacteria. This cell wall synthesis inhibitor interacts with peptidoglycan building blocks, which leads to lysis and cell death. Increased hydroxyl radical levels in *S. aureus* within 3 h post-treatment have been reported after exposure to a lethal concentration of vancomycin (5 μg mL^{-1}) compared to sublethal concentration (1 μg mL^{-1}) [25]. Grant et al. also showed that stimulating the production of reactive oxygen species (ROS) can destroy resistant strains, which could provide a promising strategy to understand the mechanisms of killing, develop therapeutics and manage infections [29]. The hypothesis that reactive species are part of the antibiotic-induced killing mechanism is widely accepted [25,27,29–31], although researchers have reported conflicting observations [32,33]. Keren et al. showed no difference in live aerobic or anaerobic bacterial cells (*Escherichia coli*) treated with various antibiotics. According to observations of cells dyed with hydroxyphenyl fluorescein (HPF), they suggested that ROS do not play a role in killing bacteria by antibiotics [33]. While most research focuses on ROS, it is known that other reactive species like reactive nitrogen species play a role too [34].

There are currently several techniques available to measure ROS in a cellular environment. One can differentiate between indirect and direct methods. The indirect methods, including measurements of desoxyribonucleic acid (DNA) damage [35] or lipid peroxidation [36], measure damage caused by radicals or ROS. However, there are many alternative pathways through which such damage can occur and thus these methods provide just a rough indication. Measuring the response of the cells to radicals rather than the radicals itself is often very specific for certain radicals [37,38]. For instance, this can be done via quantitative polymerase chain reaction (PCR) for enzymes which are responsible for stress responses. Similarly, stress responses can also be studied at the ribonucleic acid (RNA) or protein level [31]. However, these methods do not provide any spatial information at all, they are destructive and require prior knowledge about which pathways are triggered by certain radicals.

Direct methods include fluorescent dyes, which react with radicals and form a fluorescent molecule. However, most of these dyes react with reactive oxygen species (ROS), which include many non-radical species, so that the measurement is usually dominated by these. There are also a few modern dyes with specificity for certain molecules which have already been used to follow ROS production in bacteria [39,40]. These dyes are often somewhat toxic and can diffuse away from where they were created, which reduces spatial resolution [41,42].

The direct method with the greatest specificity for radicals is Electron spin resonance (ESR). Such measurements are - like our technique - sensitive to the free electron of the radical itself [43,44]. However, its usefulness is limited by relatively low sensitivity. A way to circumvent this problem is to use spin labels which react with the primary radical to form more stable radicals. These can then be detected by ESR, although the low sensitivity still limits spatial resolution.

A final limitation of all dyes and spin labels is that they measure the signal of free radicals or ROS that have accumulated over time, giving information about the history of the sample rather than a real-time representation. With this paper, we demonstrate the basis for a method that can specifically detect free radicals (i.e., not all ROS) with improved spatial resolution, time resolution and sensitivity.

2. Experimental section

In the present study, we investigated the possibility of free radical detection in a bacterial environment during stress using NV relaxometry. As illustrated in Fig. 1, we hypothesized that FNDs located at the cell walls of *S. aureus* can be used to detect free radicals that are produced at elevated levels or leaked through compromised cell walls as a result of exposure to vancomycin. While FNDs are internalized in the cytosol of mammalian cells by endocytosis pathway [45], bacterial cells are typically much smaller, and the lack of FND uptake in bacteria was already reported in our previous research studies [15,16]. The method detects the concentration of free radicals less than 100 nm around [10] a particle on the bacterial surface, including in its range the bacterial cell wall (20–40 nm) [46], the environment immediately exterior to the cell wall and potentially a small region of the cell interior.

2.1. Diamond materials

For all experiments in this study, we used fluorescent nanodiamonds (FNDs) with a median hydrodynamic diameter of 70 nm, which are commercially available from Adamas Nanotechnologies (NC, USA). These particles are produced via high pressure high temperature (HPHT) synthesis by the vendor and contain approximately 500 NV centers per particle (due to irradiation). In addition, they host oxygen groups on the surface due to oxidizing acid cleaning in the last step of fabrication. Since these fluorescent defects are protected in the crystal lattice, FNDs have the advantage that they never bleach [47]. The characterization of these particles has extensively been done in the previous literature [48].

2.2. Bacterial culturing

Staphylococcus aureus ATCC 12600, a Gram-positive bacterium with high Extracellular Polymeric Substance (EPS) excretion ability, was selected in this study. The interaction of these bacterial cells and various nanodiamond particles was investigated in our previous studies, which show good biocompatibility of cells interfaced with the nanoparticles [15,16]. As scanning electron microscopy (SEM) images have shown, nanodiamonds adhere to the outer cell surface of bacteria without any mechanical damages. *S. aureus*'s preculture was prepared by inoculating one colony from a fresh blood agar (BA) plate into 10 mL sterile Tryptic Soy Broth (TSB) followed by incubation at 37 °C for 24 h. 2.5 mL of overnight cultures were diluted into 50 mL sterile growth medium (TSB) and incubated at 37 °C for 16 h to grow the main-culture. The main-culture was then washed twice with phosphate-buffered saline (PBS) by centrifuging at 5000 g (5 min at 10 °C). To break apart bacterial aggregates, the bacterial solution subsequently was sonicated on the ice for 3 × 10 s at 30 W (Vibra Cell model VCX130; Sonics and Materials Inc., Newtown, CT, USA). The cells were then enumerated using a

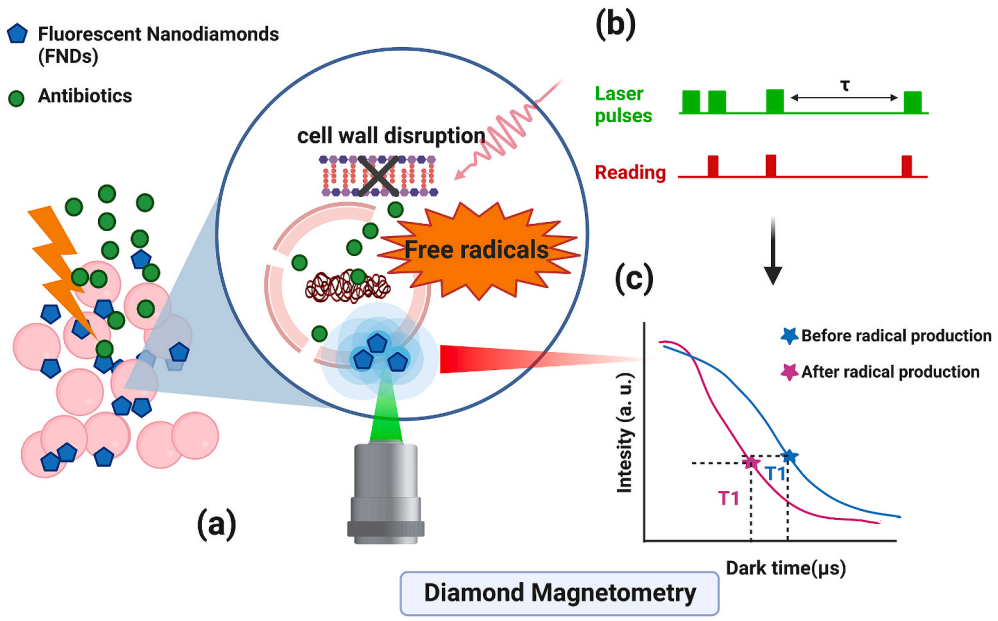

Fig. 1. Schematic diagram showing (**a**) the hypothesized radical production in *S. aureus* during antibiotics exposure and the relaxometry principle. (**b**) The green blocks indicate when the laser is on, while the red blocks indicate when we read out the photo-luminescence from the FND. (**c**) The dark times τ were varied to probe if the NV centers have returned to the darker equilibrium state. (A colour version of this figure can be viewed online.)

Bürker-Türk counting chamber. For further experiments, the concentration of bacterial suspension was adjusted to 1.0×10^9 bacteria per mL PBS.

2.3. Sample preparation for diamond magnetometry

In this study, air-plasma surface treatment was performed on glass-bottom quartered Petri dishes to produce hydrophilic functional groups on the glass surfaces [49]. The multifunctional plasma process aimed to activate the surface, promote the attraction with FNDs, and deposit them firmly and limit the nanoparticles' movement. Petri dishes were placed in an air-plasma oven (Multifunctional Plasma System commercialized by Diener electronics) and treated for 10–15 min with a low-pressure system adjusted to 0.2 mbar. Hereafter, 100 μL of FNDs (20 μg mL^{-1} in water) was deposited on the plasma-activated plates. After air-drying overnight, bacterial cells were added to the plates with FNDs and incubated at 37 °C for 2 h. Afterward, the bacterial suspension was removed slightly and rinsed once with PBS to remove poorly attached bacteria (to avoid fluorescent background from freely floating bacteria). The samples remained in 100 μL of PBS during the relaxometry measurements.

2.4. Confocal microscopy

Confocal scanning laser microscopy (CSLM) was performed to localize nanodiamonds on or distinguishingly close to the bacterial cell wall. The sample preparation was done as described above in the 2.3 section. The attached bacterial cells on the glass surface were stained with SYTO9. A Zeiss LSM 780 confocal laser scanning microscope (Zeiss, Jena, Germany) was used to analyze specimens. A 488 nm laser was used for excitation, and the emission was observed at 528 nm (SYTO9). The FNDs' NV centers were excited with a 561 nm laser, and their emission was collected from 606 to 694 nm. Zeiss ZEN software was used to acquire images.

The original confocal images (the same as previous images) were processed in FIJI software. To reduce noise and/or enhance features, first, the noise (outliers) were removed, Gamma values were adjusted to 1.10, and followed by applying a Gaussian Blur filter for all images of control (bacteria) and sample (bacteria + FNDs).

2.5. T_1 measurements

We use a specific kind of diamond magnetometry called relaxometry or T_1 measurements. To perform such a measurement, we pump the NV centers in the nanodiamonds into the (bright) $|m_s = 0>$ level of ground state using a green (532 nm) excitation laser. We then read out the magnetic state again after varying dark times τ (from 0.2 μs to 10 ms). In the presence of spin noise produced by radicals, the NV centers' magnetic state returns more quickly to the thermal equilibrium between $|m_s = 0>$ and $|m_s = \pm 1>$ with a lower fluorescence intensity. The characteristic time T_1 parameter of this relaxation process provides a measure for the free radical concentration. The signal is analogous to T_1 in conventional MRI but obtained from nanoscale voxels.

To perform the measurements, we use a home-built magnetometry setup, which has been described in previous work [50]. The setup is a confocal microscope which allows laser pulsing and readout at specific timings. A 100x magnification oil objective (Olympus, UPLSAPO 100XO) was used for light collection. An acousto-optical modulator (Gooch & Housego, model 3350-199) was implemented to conduct the pulsing sequence. The length of each pulse was set to 5 μs to ensure the polarization of the NV centers. While each T_1 sequence takes on the order of microseconds, we typically repeated the sequence 10,000 times for each measurement in order to obtain a sufficient signal-to-noise ratio. The total time such T_1 measurements took was around 10 min. A tracking algorithm was used to track the movement of a diamond particle on the cell surface to ensure it remained in focus. The 532 nm green laser (CNI, Changchun, China) was attenuated to 50 μW at the location of the sample. An avalanche photodiode (APD) was used to detect single photons at wavelengths longer than 600 nm.

First, we performed measurements of the initial condition for 40 min and then performed an intervention (adding different vancomycin concentrations at the common range or ultra violet (UV) light at 275 nm, 23.7 mW cm^{-2}) and measured T_1 afterward for 90 min to observe changes. The concentrations applied may seem high with respect to the MIC values measured for 10^5 CFU mL^{-1} of *S. aureus* ATCC 12600 (2 μg mL^{-1}) [51] but were inspired by the common concentration range chosen by researchers for the higher bacterial inoculum [26,52,53].

2.6. Fluorescence Microscopy for Testing the Effect of Antibiotics on S. aureus

After testing the initial bacterial adhesion on the glass surfaces, we studied the effect of antibiotics on *S. aureus* by adding the various concentrations of vancomycin to bacterial cells seeded for 2 h. These cultures were incubated for 90 min after treatment, and cellular growth was scored by performing a LIVE/DEAD™ BacLight™ Bacterial Viability Assay (Invitrogen, USA) before and after treatment with different vancomycin concentrations and H_2O_2 (see Supplementary Information Fig. S1). The live/dead staining solution is prepared by mixing components SYTO9 and propidium iodide (PI) with a 1:1 ratio. After adding the staining solution, samples are incubated for 15 min at room temperature in the dark [54]. The cells were imaged by fluorescence microscopy (Leica Microsystems CMS GmbH, Type DM4000B, Camera: Leica DFC350×, 40× water objective).

2.7. Fluorescent dye-based determination of ROS production

We compared magnetometry data with the results obtained by an established technique for measuring intracellular Reactive Oxygen Species (ROS) in bacteria upon antibiotic treatment. ROS production in bacteria was measured by using the H_2DCFDA kit (Thermofisher, the Netherlands). Bacterial cultures were exposed to 2′,7′-dichlorodihydrofluorescein diacetate (H_2DCFDA) described by H. Van Acker (2016) with some modifications [55]. The cells were treated with 0.5% H_2O_2; MiliQ-water; FNDs (70 nm, 20 μg mL^{-1}); Vancomycin 20 × MIC (20 μg mL^{-1}) and cells without treatment were used as control samples. The fluorescence intensity was measured by a microplate reader (Fluostar optima, Germany) at excitation/emission of 485/540 nm at different incubation time points (0, 30, and 60 min) after adding chemicals. Three wells were included per condition, and each experiment was repeated in quadruplicate.

2.8. Statical analysis

T_1 raw data were processed by MATLAB. Statical significance was evaluated with GraphPad Prism 8.0.1 software by two-way analysis of variance (ANOVA). All data are reported as the mean value ± standard deviation (s.d.) with at least 3 independent repetition runs, followed by T-test. $P \leq 0.05$ was defined as statistically significant.

3. Result and discussion

3.1. Relaxometry for measuring free radicals generated upon stress treatments

Confocal images in Fig. 2 show FND positions and confirm that FNDs attach to the bacterial cell wall or accumulate close to *S. aureus* cells. This is also in agreement with SEM images in our previous papers [15, 16].

The T_1 in the initial state of the samples was measured for 40 min before the intervention. Recording T_1 in the post-intervention state was started immediately after adding different antibiotic concentrations

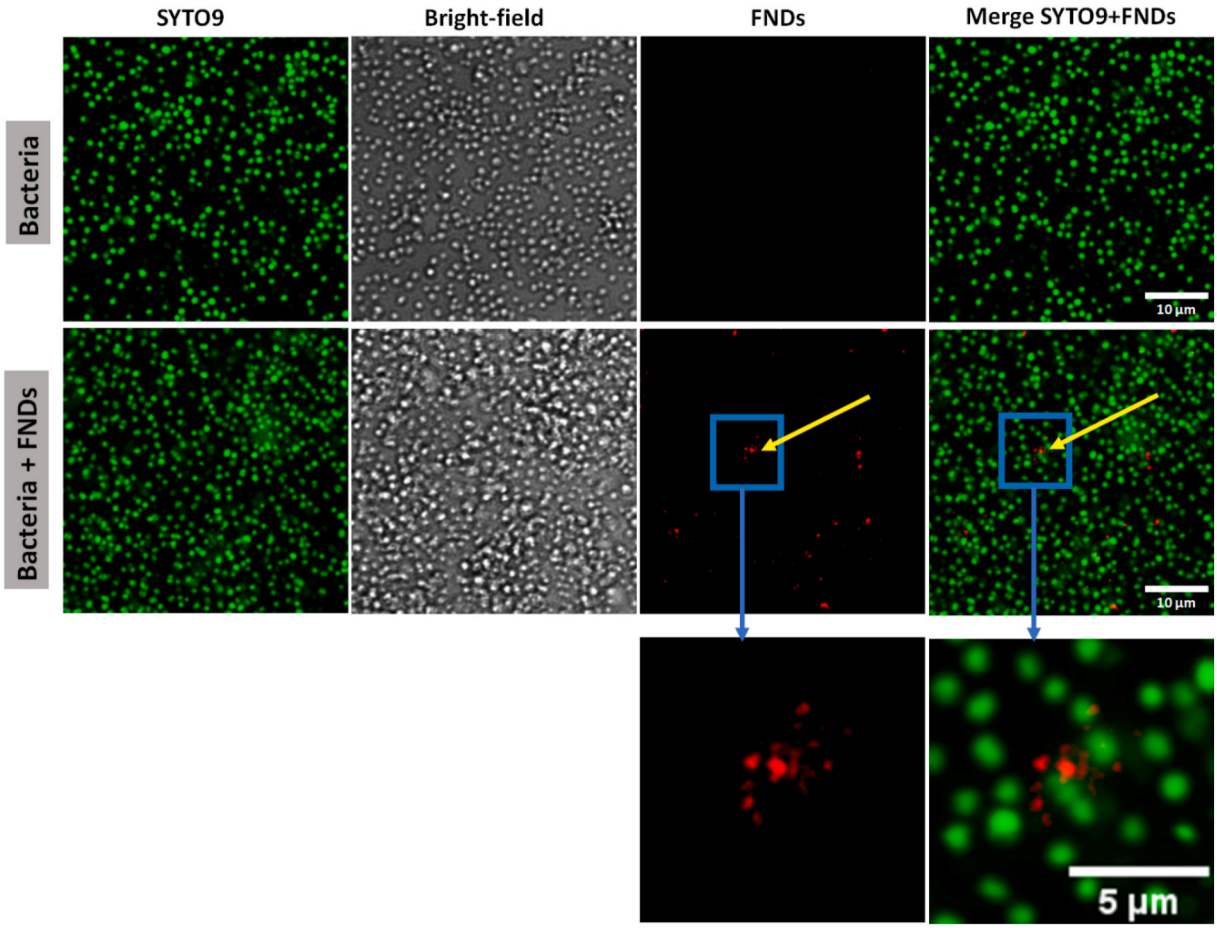

Fig. 2. Representative confocal images of FNDs + bacteria and bacteria without FNDs. *S. aureus* cells incubated for 2 h with nanodiamond particles(20 μg mL^{-1} in water) were stained with SYTO9 to be visualized by green. Gray: *S. aureus* bright field. Red: FNDs, the yellow arrows indicate FNDs position(signal) (no signal in control sample). Arrows and zoomed-in images are used to indicate nanodiamond locations which are mainly attached to or next to the bacteria. (A colour version of this figure can be viewed online.)

(2.6, 10, 20, and 340 μg mL^{-1} of final concentrations), Milli-Q water and PBS. For the control sample, T_1 was measured in absence of bacteria to observe the biological intervention's effect (Fig. 3.).

Fig. 3 shows the relative change of T_1 values measured from FNDs on bacterial cells treated with various antibiotic concentrations compared to untreated bacterial cells. As expected, T_1 values were significantly lower when the bacteria were treated with higher doses of vancomycin (20 and 340 μg mL^{-1}) than when they were treated with lower concentrations (2.6 and 10 μg mL^{-1}) or untreated (PBS). This change can be attributed to free radical production in single bacterial cells and as shown in Fig. 3, the radical generation could be dose-dependent.

To study the dynamics of free radical generation induced by antibiotics, we exposed *S. aureus* ATCC 12600 to different vancomycin concentrations for 90 min. PBS was used as a medium for untreated samples to avoid fluorescent background from the components of the bacterial growth medium. It was confirmed by recent preceding studies that there is no effect of PBS on the sensitivity of FNDs' sensing performance [12]. The differences in normalized T_1 (in percent) are shown in Fig. 4. A decrease in T_1 indicates an increased free radical concentration surrounding the FNDs induced by the drug. Over the course of 90 min of antibiotic treatment (following individual cells over the course of the entire experiment), T_1 dropped significantly. At the same time, the values of T_1 remained constant in untreated samples. The above-mentioned results agree with observations presented in Fig. 3. Additionally, higher doses lead to a faster response. While at the largest concentration (340 μg mL^{-1}), the full response is already established after 30 min, it takes the entire 90 min to establish a similar response at 10 μg mL^{-1}.

It is well established that bacteria are susceptible to UV irradiation which leads to structural cell damages by two main types of photosensitization processes. The type I mechanism involves the oxidation/reduction of one electron resulting in free radical formation. In the Type II damage process, energy transfers from the sensitizer, which absorbed the UV light directly, to an oxygen molecule resulting in an excited state of singlet oxygen [56]. These processes lead to biological damage, including cell death and mutation, by providing favorable conditions for producing highly harmful free radicals.

However, the biological effects of UV radiation of different wavelengths (UVA, UVB, and UVC) may differ greatly in different bacterial isolates. This depends on several factors, such as the efficiency of defense and repair strategies to cope with UV-induced damage or the relative combination of different ROS involved in eliciting damage [57]. It has been suggested that Gram-positive bacteria are better adapted to UV stress due to their cell walls filtering out a notable fraction of UV radiation [57]. In particular, the effect of shorter wavelength UV (UVC) causes the highest direct interaction with DNA, a major target biomolecule of UV radiation, which is in accordance with their mutagenic nature as well as antibacterial potential [57,58]. The exposure to longer wavelengths (UVA) has more subtle biological effects, attributed to indirectly enhanced production of ROS, which results in oxidative damage to lipids, proteins, and DNA. Oxidative damage upon UVB exposure was observed, which comprises elements from both direct and indirect pathways of damage [57,58]. Although UVC causes direct damage to DNA and is less related to the production of oxidative damage, it has been recently found that oxidative stress was also crucial for cell inactivation under UVC irradiation [57]. However, most studies that address the cellular effects of UV radiation make use of indirect detection methods by measuring the response of a cell or damage caused by radicals.

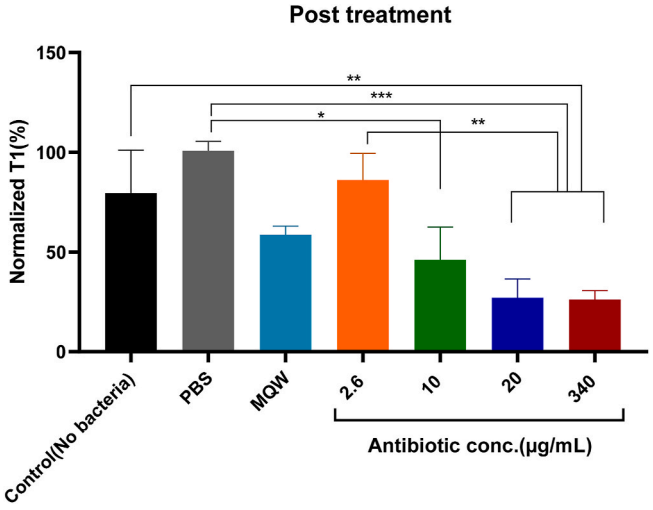

Fig. 3. Comparison of T_1 values in the presence of different treatment conditions. The T_1 value of each experiment was normalized to the initial T_1 measurement in PBS. Lower T_1 values indicate an increase in radical formation. **Control (No bacteria)** = FNDs without bacteria, and **MQW** = Milli-Q water. The experiments were repeated 3 times and error bars represent standard deviations. *P ≤ 0.05, **P ≤ 0.01 and ***P ≤ 0.001.

We studied the bacterial stress response to UV light (UVC, 200–280 nm) by conducting the same T_1 experiments. Such information is crucial to understand the role of UV radiation in UV-based disinfection strategies targeting a broad range of bacteria. The results are also plotted in Fig. 4. We observed a decrease in T_1 during 90 min of UV irradiation. At first, there were no statistically significant differences between T_1 in untreated and UV-treated samples, while this changed significantly ($p < 0.01$) after 1 h. The differences observed in T_1 for UV-treated and antibiotic-treated samples (at 20 and 340 μg mL^{-1}) were significant at the beginning ($p < 0.001$). However, at the end of treatment, T_1 remained constant, which can be the result of saturation of the treatment's effect or reaching the time resolution limit of the equipment. Below a threshold relaxation time, our equipment is unable to differentiate shorter T_1 values since the minimal time interval between pulses we can generate is reached. This could be resolved by using equipment with a faster pulse rate. Saturation of the antibacterial effect of increased antibiotic doses would agree with observations in the live-dead stain experiments presented in Fig. 5. In general, our relaxometry results are consistent, and T_1 decreasing was continuous after adding antibiotics. UV-treated cells show slightly higher T_1 and a significant decrease in T_1 was measured after 1 h of treatment. This suggests that UVC light has less influence on free radical generation in bacterial cells than lethal doses of antibiotics.

The results of the present study confirmed that the lack of FND uptake by bacterial cells does not exclude relaxometry as an applicable method in microbiology, providing a valuable strategy for free radical detection. Since the NDs are outside of the bacterial cells, the increase in detected free radicals might be the result of lysis/destruction of the bacterial cell wall by antibiotics causing intracellular free radicals to leak out and come in contact with the ND, causing T_1 to decrease. As this reduction was dose dependent, relaxometry allowed us to differentiate between free radical levels in different antibiotic concentrations and UV treatment. Apart from obtaining qualitative information, it is also possible to calibrate relaxometry data with known radical concentrations in a controlled environment [12]. Based on radical measurements under controlled conditions the concentrations we observe here are in the nanomolar range [12].

The results of this study demonstrate that relaxometry can be used to perform a measurement before and during intervention on the exact same cell and the exact same particle, similar to what has been shown previously in other cell types [12,14]. Additionally, we have shown that the sensitivity of relaxometry is sufficient to detect free radicals [12].

To give our data full consideration, it should be noted that the paramagnetic form of iron might also have an influence on T_1. However, since we did our experiments in PBS, we did not include iron compounds, such as were seen by Wang et al. [44] in electron spin resonance (ESR) spectroscopy. Wang et al. have also measured the internal iron

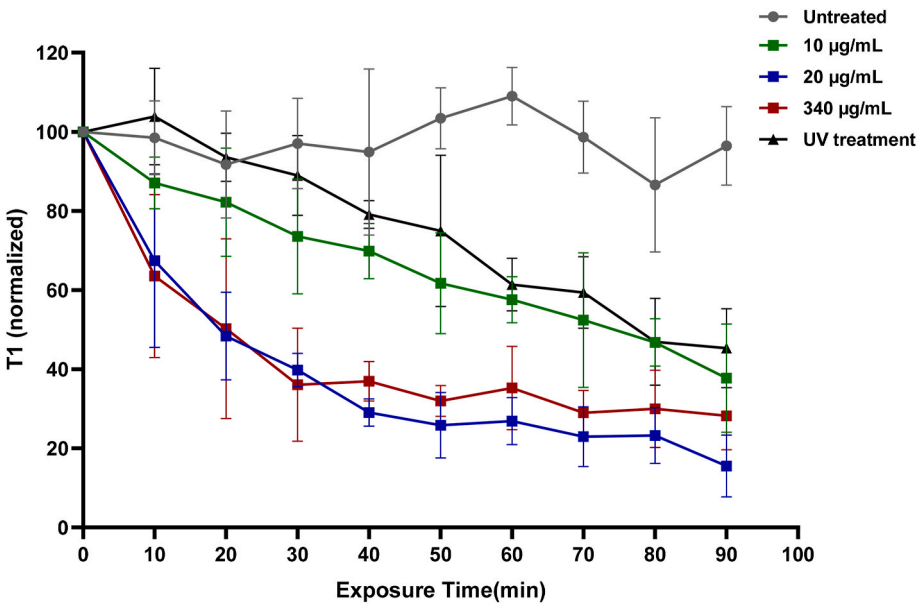

Fig. 4. Dynamical radical detection in single *S. aureus* cells by T_1 measurements. The cells were treated with the antibiotic (vancomycin different lethal doses) and UV irradiation (time post-treatment = 0–90 min). Untreated samples represented bacterial cells in PBS were considered as control samples. The experiments were repeated 3 times, and error bars represent standard deviations.

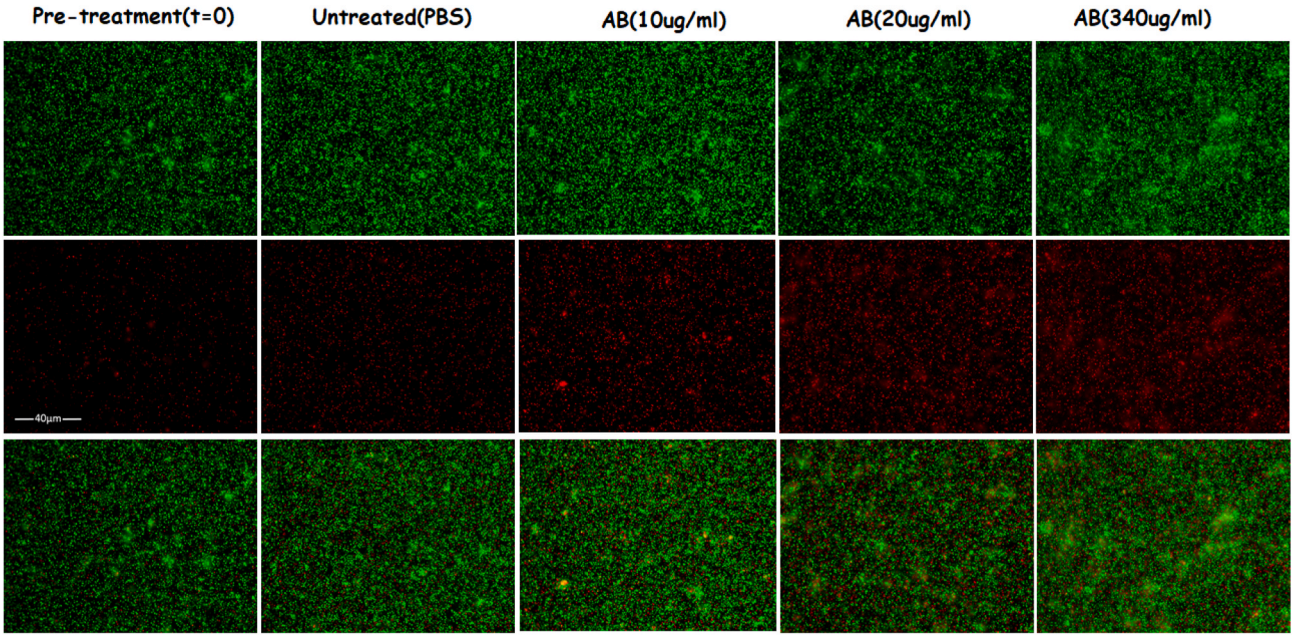

Fig. 5. Evaluation of live/dead staining of *S. aureus* following treatment for 90 min with three concentrations of vancomycin (**AB** = antibiotic) measured by fluorescent microscopy using SYTO9 green-fluorescent stain (live organisms) and PI red-fluorescent stain (dead organisms). Pre-treatment samples contained *S. aureus* cells on glass surfaces before adding chemicals. Untreated samples represented bacterial cells treated by PBS. **Note**: All images were taken at 40 × magnification. (A colour version of this figure can be viewed online.)

concentration of *S. aureus* with and without 6 h of antibiotic treatment (2.5 μg ml^{-1} vancomycin or 0.4 μg ml^{-1} ciprofloxacin), and they did not find any significant differences in iron concentration in the supernatant from antibiotic treated compared to untreated samples. Thus, we do not expect significant iron release by using higher concentration of vancomycin.

3.2. Live-dead staining

To compare our relaxation measurements with established methods, a live-dead assay of *S. aureus* ATCC 12600 strain was performed following treatment for 90 min with various conditions. The resulting images are presented in Fig. 5 and show the effect of vancomycin used at lethal concentrations compared to pre-treated and untreated samples. We observed an increase in the number of dead cells, which was antibiotic concentration dependent. Also, in the control sample, after adding PBS instead of antibiotic, both live and dead bacteria are present after 2 h. Nevertheless, the number of dead cells is much lower than on the treated surfaces, which shows a similar trend as our observations in the relaxation measurements (shown in Fig. 4). Fluorescence imaging of

S. aureus shows no significant difference in the number of dead cells in samples treated by antibiotics and H_2O_2 (a positive control), observationally. However, the number of dead cells in both samples markedly increased compared to control samples (see Supplementary Information Fig. S1.).

3.3. Comparing to ROS measurements by fluorescent-based probe

As mentioned earlier, there are some fluorescent dye-based methods to detect ROS generation in bacteria. We chose to investigate the sensitivity of one of these methods compared to our relaxometry-based approach. According to the literature, the conventional H_2DCFDA assay is a sensitive, direct, non-specific ROS detection method [55]. As a positive control, bacterial cells were exposed to 0.5% H_2O_2. At the initial measurement (t = 0) there were no significant differences in the fluorescence intensity between samples treated with antibiotics, Milli-Q water and FNDs. Almost no trend is visible for other time points. As expected, ROS production was only statistically significant for the positive control samples treated by H_2O_2 ($p < 0.0001$). The results are shown in Fig. 6 suggest that the investigated conventional method was not sensitive enough to measure ROS generated in *S. aureus* during antibiotic treatment. We also do not see any differences between fluorescence intensities from the control and the FND group. This confirms that, with the sensitivity of this method, no detectable ROS production caused by the presence of diamond particles themselves can be detected.

It is worth revisiting that there are important differences between conventional assays and relaxometry. The two assays differ in when, where, and what they measure as outputs [14]. Our diamond-based relaxometry method measures local changes at the scale of single cells, while H_2DCFDA measures a larger population. It also detects (paramagnetic) free radicals, whereas H_2DCFDA measures all ROS, most of which are not radicals. Furthermore, the fluorescent dye can diffuse and thus, the signals can come from a location that is not necessarily where the radicals were created. A way to circumvent limited spatial resolution was demonstrated by Yi et al. They use specific inhibitors and then compare the ROS production with a control [59]. However, this approach requires that there is a very efficient inhibitor that is not toxic and that it is known which process needs to be inhibited. Fluorescent nanodiamonds on the other hand are only sensitive to radicals in their immediate surrounding (up to some tens of nanometer). Thus, if the cells are a few micrometers apart, as is the case here, the nanodiamonds are likely to only detect radicals from single cells. Most radicals are so short lived that they are destroyed before they can diffuse a few microns and even the most long-lived radicals are drastically reduced a few microns away from the cell surface [60]. Moreover, dyes like H_2DCFDA measure the history of the sample while the FND measurements before and after from the same cells at the same location, and the data are collected in real-time. Finally, the relevant conventional method needs several steps for pre-treatment, and the results vary with experimental conditions. Relaxometry measurements are relatively insensitive to pH and temperature in the relevant range [14]. In addition, ESR/spin trapping was examined as an approach to monitor the intracellular and extracellular free radical formation in *S. aureus* while treating with antibiotics (vancomycin or ciprofloxacin) [44]. However, the method is relatively insensitive and requires relatively high concentrations of spin traps.

4. Conclusion

Measuring free radicals is challenging due to their short half-life and low steady-state concentration. There are several distinct features of our technique that are complementary to existing techniques. Our method measures the current radical load while fluorescent probes measure the accumulated ROS over the history of the sample. Our readout is local and comes from the area below 100 nm around the particle while the readout from the fluorescent probes is usually from the entire sample or at least a large ensemble. Most fluorescent probe based techniques

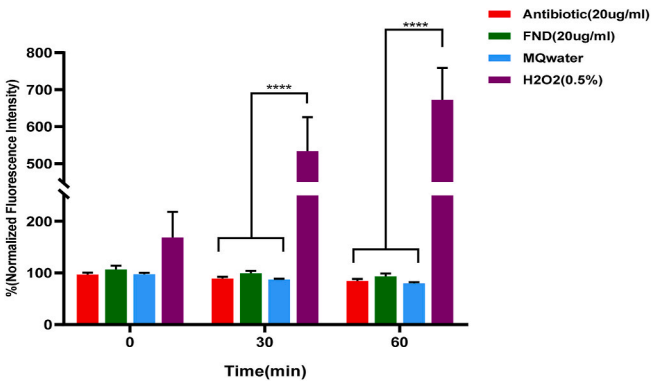

Fig. 6. Fluorescence generated over time (0–60 min) in treated bacterial cells with antibiotic (**AB**:20 μg mL^{-1}), Milli-Q water (**MQw**), fluorescent nanodiamonds (**FND**:20 μg mL^{-1}) and **H_2O_2** (0.5%). Mean values (n = 4) were expressed as normalized % of the fluorescence signal of their control. The experiments were repeated 4 times and error bars represent standard deviations and ****P ≤ 0.0001.

(including DCFDA) measure different chemicals and are also sensitive to non-paramagnetic species like H_2O_2. Since these are about an order of magnitude more abundant, they will dominate the readout. On the other hand, diamond-based relaxometry does not detect H_2O_2 at all, since it is sensitive to the unpaired electron of radicals. It is essentially an ESR signal with greater sensitivity and spatial resolution. Depending on the quantities and qualities of interest, this may be an advantage or a drawback. In addition, while fluorescent probes bleach over time, FNDs are infinitely stable, allowing for continuous long term measurements on the same cell and same particle.

We report here that exposing bacterial cells to stress conditions leads to a dose dependent free radical response, which correlates with the killing of bacterial cells of *S. aureus*. We further observed the dynamics of radical generation at the single-cell level. This kind of information is valuable for assessing the working mechanisms of bacterial killing as well as the formation of resistance.

CRediT authorship contribution statement

Neda Norouzi: have conducted the experimental work. The article was written edited by all the authors. All authors have approved the final version of the article. **Anggrek Citra Nusantara:** has conducted the experimental work. **Yori Ong:** assisted the experimental work. **Thamir Hamoh:** assisted the experimental work. **Linyan Nie:** assisted the experimental work. **Aryan Morita:** assisted the experimental work. **Yue Zhang:** assisted the experimental work. **Aldona Mzyk:** Co-supervised the project. **Romana Schirhagl:** Supervised the project.

Declaration of competing interest

The authors declare the following financial interests/personal relationships which may be considered as potential competing interests: Yue Zhang and Linyan Nie report financial support was provided by the Chinese scholarship council. Aryan Morita reports financial support was provided by LPDP.

Acknowledgments

We would like to acknowledge funding from LPDP for Aryan Morita as well as from the Chinese scholarship council for a scholarship for Linyan Nie and Yue Zhang. Neda Norouzi and Anggrek Citra Nusantara contributed equally to this work.

Appendix A. Supplementary data

Supplementary data to this article can be found online at https://doi.org/10.1016/j.carbon.2022.08.025.

References

[1] L. Rondin, J.-P. Tetienne, S. Rohart, A. Thiaville, T. Hingant, P. Spinicelli, J.-F. Roch, V. Jacques, Stray-field imaging of magnetic vortices with a single diamond spin, Nat. Commun. 4 (1) (2013) 2279, https://doi.org/10.1038/ncomms3279.

[2] D. Le Sage, K. Arai, D.R. Glenn, S.J. DeVience, L.M. Pham, L. Rahn-Lee, M.D. Lukin, A. Yacoby, A. Komeili, R.L. Walsworth, Optical magnetic imaging of living cells, Nature 496 (7446) (2013) 486–489, https://doi.org/10.1038/nature12072.

[3] M. Loretz, S. Pezzagna, J. Meijer, C.L. Degen, Nanoscale nuclear magnetic resonance with a 1.9-nm-deep nitrogen-vacancy sensor, Appl. Phys. Lett. 104 (3) (2014), https://doi.org/10.1063/1.4862749, 033102.

[4] H.J. Mamin, M. Kim, M.H. Sherwood, C.T. Rettner, K. Ohno, D.D. Awschalom, D. Rugar, Nanoscale nuclear magnetic resonance with a nitrogen-vacancy spin sensor, Science 339 (6119) (2013) 557–560, https://doi.org/10.1126/science.1231540.

[5] T. Staudacher, F. Shi, S. Pezzagna, J. Meijer, J. Du, C.A. Meriles, F. Reinhard, J. Wrachtrup, Nuclear magnetic resonance spectroscopy on a (5-nanometer)3 sample volume, Science 339 (6119) (2013) 561–563, https://doi.org/10.1126/science.1231675.

[6] S.R. Hemelaar, B. Saspaanithy, S.R.M. L'Hommelet, F.P. Perona Martinez, K.J. Van der Laan, R. Schirhagl, The response of HeLa cells to fluorescent NanoDiamond uptake, Sensors 18 (2) (2018) 355, https://doi.org/10.3390/s18020355.

[7] V. Vaijayanthimala, P.-Y. Cheng, S.-H. Yeh, K.-K. Liu, C.-H. Hsiao, J.-I. Chao, H.-C. Chang, The long-term stability and biocompatibility of fluorescent nanodiamond as an in vivo contrast agent, Biomaterials 33 (31) (2012) 7794–7802, https://doi.org/10.1016/j.biomaterials.2012.06.084.

[8] S. Rojas, J.D. Gispert, R. Martín, S. Abad, C. Menchón, D. Pareto, V.M. Víctor, M. Alvaro, H. García, J.R. Herance, Biodistribution of amino-functionalized diamond nanoparticles. In vivo studies based on 18F radionuclide emission, ACS Nano 5 (7) (2011) 5552–5559, https://doi.org/10.1021/nn200986z.

[9] L.-W. Tsai, Y.-C. Lin, E. Perevedentseva, A. Lugovtsov, A. Priezzhev, C.-L. Cheng, Nanodiamonds for medical applications: interaction with blood in vitro and in vivo, Int. J. Mol. Sci. 17 (7) (2016) 1111, https://doi.org/10.3390/ijms17071111.

[10] M. Pelliccione, B.A. Myers, L.M.A. Pascal, A. Das, A.C. Bleszynski Jayich, Two-dimensional nanoscale imaging of gadolinium spins via scanning probe relaxometry with a single spin in diamond, Physical Review Applied 2 (5) (2014) 1–7, https://doi.org/10.1103/PhysRevApplied.2.054014.

[11] J.P. Tetienne, T. Hingant, L. Rondin, A. Cavaillès, L. Mayer, G. Dantelle, T. Gacoin, J. Wrachtrup, J.F. Roch, V. Jacques, Spin relaxometry of single nitrogen-vacancy defects in diamond nanocrystals for magnetic noise sensing, Phys. Rev. B Condens. Matter 87 (23) (2013) 1–13, https://doi.org/10.1103/PhysRevB.87.235436.

[12] F. Perona Martínez, A.C. Nusantara, M. Chipaux, S.K. Padamati, R. Schirhagl, Nanodiamond relaxometry-based detection of free-radical species when produced in chemical reactions in biologically relevant conditions, ACS Sens. 5 (12) (2020) 3862–3869, https://doi.org/10.1021/acssensors.0c01037.

[13] A. Morita, T. Hamoh, A. Sigaeva, N. Norouzi, A. Nagl, K.J. van der Laan, E.P. P. Evans, R. Schirhagl, Targeting nanodiamonds to the nucleus in yeast cells, Nanomaterials 10 (10) (2020) 1962, https://doi.org/10.3390/nano10101962.

[14] L. Nie, A.C. Nusantara, V.G. Damle, R. Sharmin, E.P.P. Evans, S.R. Hemelaar, K. J. van der Laan, R. Li, F.P.P. Martinez, T. Vedelaar, M. Chipaux, R. Schirhagl, Quantum monitoring of cellular metabolic activities in single mitochondria, Sci. Adv. 7 (21) (2021), eabf0573, https://doi.org/10.1126/sciadv.abf0573.

[15] S.Y. Ong, R.J.J. van Harmelen, N. Norouzi, F. Offens, I.M. Venema, M.B. Habibi Najafi, R. Schirhagl, Interaction of nanodiamonds with bacteria, Nanoscale 10 (36) (2018) 17117–17124, https://doi.org/10.1039/C8NR05183F.

[16] N. Norouzi, Y. Ong, V.G. Damle, M.B. Habibi Najafi, R. Schirhagl, Effect of medium and aggregation on antibacterial activity of nanodiamonds, Mater. Sci. Eng. C 112 (2020), 110930, https://doi.org/10.1016/j.msec.2020.110930.

[17] J. Wehling, R. Dringen, R.N. Zare, M. Maas, K. Rezwan, Bactericidal activity of partially oxidized nanodiamonds, ACS Nano 8 (6) (2014) 6475–6483, https://doi.org/10.1021/nn502230m.

[18] J. Beranová, G. Seydlová, H. Kozak, Š. Potocký, I. Konopásek, A. Kromka, Antibacterial behavior of diamond nanoparticles against Escherichia coli, Physica Status Solidi (B) Basic Research 249 (12) (2012) 2581–2584, https://doi.org/10.1002/pssb.201200079.

[19] J. Beranová, G. Seydlová, H. Kozak, O. Benada, R. Fišer, A. Artemenko, I. Konopásek, A. Kromka, Sensitivity of bacteria to diamond nanoparticles of various size differs in gram-positive and gram-negative cells, FEMS (Fed. Eur. Microbiol. Soc.) Microbiol. Lett. 351 (2) (2014) 179–186, https://doi.org/10.1111/1574-6968.12373.

[20] NIH, National Institute of Allergy and Infectious Diseases | Leading research to understand, treat, and prevent infectious, immunologic, and allergic diseases. https://www.niaid.nih.gov/. (Accessed 20 November 2020).

[21] X. Liu, M. Marrakchi, M. Jahne, S. Rogers, S. Andreescu, Real-time investigation of antibiotics-induced oxidative stress and superoxide release in bacteria using an electrochemical biosensor, Free Radic. Biol. Med. 91 (2016) 25–33, https://doi.org/10.1016/j.freeradbiomed.2015.12.001.

[22] L. Ma, Y. Gao, A.W. Maresso, Escherichia coli free radical-based killing mechanism driven by a unique combination of iron restriction and certain antibiotics, J. Bacteriol. 197 (23) (2015) 3708–3719, https://doi.org/10.1128/JB.00758-15.

[23] R.S. Ray, S. Mehrotra, U. Shankar, G.S. Babu, P.C. Joshi, R.K. Hans, Evaluation of uv-induced superoxide radical generation potential of some common antibiotics, Drug Chem. Toxicol. 24 (2) (2001) 191–200, https://doi.org/10.1081/DCT-100102610.

[24] V.V. Loi, N.T.T. Huyen, T. Busche, Q.N. Tung, M.C.H. Gruhlke, J. Kalinowski, J. Bernhardt, A.J. Slusarenko, H. Antelmann, Staphylococcus aureus responds to allicin by global S-thioallylation – role of the brx/BSH/YpdA pathway and the disulfide reductase MerA to overcome allicin stress, Free Radic. Biol. Med. 139 (2019) 55–69, https://doi.org/10.1016/j.freeradbiomed.2019.05.018.

[25] M.A. Kohanski, D.J. Dwyer, B. Hayete, C.A. Lawrence, J.J. Collins, A common mechanism of cellular death induced by bactericidal antibiotics, Cell 130 (5) (2007) 797–810, https://doi.org/10.1016/j.cell.2007.06.049.

[26] H. Van Acker, T. Coenye, The role of reactive oxygen species in antibiotic-mediated killing of bacteria, Trends Microbiol. 25 (6) (2017) 456–466, https://doi.org/10.1016/j.tim.2016.12.008.

[27] D.J. Dwyer, M.A. Kohanski, J.J. Collins, Role of reactive oxygen species in antibiotic action and resistance, Curr. Opin. Microbiol. 12 (5) (2009) 482–489, https://doi.org/10.1016/j.mib.2009.06.018.

[28] C. Nathan, A. Cunningham-Bussel, Beyond oxidative stress: an immunologist's guide to reactive oxygen species, Nat. Rev. Immunol. 13 (5) (2013) 349–361, https://doi.org/10.1038/nri3423.

[29] S.S. Grant, B.B. Kaufmann, N.S. Chand, N. Haseley, D.T. Hung, Eradication of bacterial persisters with antibiotic-generated hydroxyl radicals, Proc. Natl. Acad. Sci. U.S.A. 109 (30) (2012) 12147–12152, https://doi.org/10.1073/pnas.1203735109.

[30] M.A. Kohanski, D.J. Dwyer, J.J. Collins, How antibiotics kill bacteria: from targets to networks, Nat. Rev. Microbiol. 8 (6) (2010) 423–435, https://doi.org/10.1038/nrmicro2333.

[31] D.J. Dwyer, P.A. Belenky, J.H. Yang, I.C. MacDonald, J.D. Martell, N. Takahashi, C. T.Y. Chan, M.A. Lobritz, D. Braff, E.G. Schwarz, J.D. Ye, M. Pati, M. Vercruysse, P. S. Ralifo, K.R. Allison, A.S. Khalil, A.Y. Ting, G.C. Walker, J.J. Collins, Antibiotics induce redox-related physiological alterations as part of their lethality, Proc. Natl. Acad. Sci. USA 111 (20) (2014) E2100–E2109, https://doi.org/10.1073/pnas.1401876111.

[32] J.A. Imlay, Diagnosing oxidative stress in bacteria: not as easy as you might think, Curr. Opin. Microbiol. 24 (2015) 124–131, https://doi.org/10.1016/j.mib.2015.01.004.

[33] I. Keren, Y. Wu, J. Inocencio, L.R. Mulcahy, K. Lewis, Killing by bactericidal antibiotics does not depend on reactive oxygen species, Science 339 (6124) (2013) 1213–1216, https://doi.org/10.1126/science.1232688.

[34] F. Vatansever, W.C.M.A. de Melo, P. Avci, D. Vecchio, M. Sadasivam, A. Gupta, R. Chandran, M. Karimi, N.A. Parizotto, R. Yin, G.P. Tegos, M.R. Hamblin, Antimicrobial strategies centered around reactive oxygen species – bactericidal antibiotics, photodynamic therapy, and beyond, FEMS (Fed. Eur. Microbiol. Soc.) Microbiol. Rev. 37 (6) (2013) 955–989, https://doi.org/10.1111/1574-6976.12026.

[35] Y.-Y. He, D.-P. Häder, UV-B-Induced formation of reactive oxygen species and oxidative damage of the cyanobacterium anabaena sp.: protective effects of ascorbic acid and N-Acetyl-l-Cysteine, J. Photochem. Photobiol. B Biol. 66 (2) (2002) 115–124, https://doi.org/10.1016/S1011-1344(02)00231-2.

[36] J.M. Pérez, I.L. Calderón, F.A. Arenas, D.E. Fuentes, G.A. Pradenas, E.L. Fuentes, J. M. Sandoval, M.E. Castro, A.O. Elías, C.C. Vásquez, Bacterial toxicity of potassium tellurite: unveiling an ancient enigma, PLoS One 2 (2) (2007) e211, https://doi.org/10.1371/journal.pone.0000211.

[37] S.Y. Boo, C.M.V.L. Wong, K.F. Rodrigues, N. Najimudin, A.M.A. Murad, N. M. Mahadi, Thermal stress responses in antarctic yeast, glaciozyma Antarctica PI12, characterized by real-time quantitative PCR, Polar Biol. 36 (3) (2013) 381–389, https://doi.org/10.1007/s00300-012-1268-2.

[38] N. Desroche, C. Beltramo, J. Guzzo, Determination of an internal control to apply reverse transcription quantitative PCR to study stress response in the lactic acid bacterium oenococcus oeni, J. Microbiol. Methods 60 (3) (2005) 325–333, https://doi.org/10.1016/j.mimet.2004.10.010.

[39] S.R. Martínez, A.M. Durantini, M.C. Becerra, G. Cosa, Real-time single-cell imaging reveals accelerating lipid peroxyl radical formation in Escherichia coli triggered by a fluoroquinolone antibiotic, ACS Infect. Dis. 6 (9) (2020) 2468–2477, https://doi.org/10.1021/acsinfecdis.0c00317.

[40] L. Wu, A.C. Sedgwick, X. Sun, S.D. Bull, X.-P. He, T.D. James, Reaction-based fluorescent probes for the detection and imaging of reactive oxygen, nitrogen, and sulfur species, Acc. Chem. Res. 52 (9) (2019) 2582–2597, https://doi.org/10.1021/acs.accounts.9b00302.

[41] Z. Wang, K. Yi, Q. Lin, L. Yang, X. Chen, H. Chen, Y. Liu, D. Wei, Free radical sensors based on inner-cutting graphene field-effect transistors, Nat. Commun. 10 (1) (2019) 1544, https://doi.org/10.1038/s41467-019-09573-4.

[42] P. Wardman, Fluorescent and luminescent probes for measurement of oxidative and nitrosative species in cells and tissues: progress, pitfalls, and prospects, Free Radic. Biol. Med. 43 (7) (2007) 995–1022, https://doi.org/10.1016/j.freeradbiomed.2007.06.026.

[43] I. Spasojević, Free radicals and antioxidants at a glance using EPR spectroscopy, Crit. Rev. Clin. Lab Sci. 48 (3) (2011) 114–142, https://doi.org/10.3109/10408363.2011.591772.

[44] Y. Wang, A.B. Hougaard, W. Paulander, L.H. Skibsted, H. Ingmer, M.L. Andersen, Catalase expression is modulated by vancomycin and ciprofloxacin and influences

the formation of free radicals in Staphylococcus aureus cultures, Appl. Environ. Microbiol. 81 (18) (2015) 6393–6398, https://doi.org/10.1128/AEM.01199-15.
[45] S.R. Hemelaar, K.J. van der Laan, S.R. Hinterding, M.V. Koot, E. Ellermann, F. P. Perona-Martinez, D. Roig, S. Hommelet, D. Novarina, H. Takahashi, M. Chang, R. Schirhagl, Generally applicable transformation protocols for fluorescent nanodiamond internalization into cells, Sci. Rep. 7 (1) (2017) 5862, https://doi.org/10.1038/s41598-017-06180-5.
[46] P. Giesbrecht, T. Kersten, H. Maidhof, J. Wecke, Staphylococcal cell wall: morphogenesis and fatal variations in the presence of penicillin, Microbiol. Mol. Biol. Rev. 62 (4) (1998) 1371–1414, https://doi.org/10.1128/MMBR.62.4.1371-1414.1998.
[47] K. van der Laan, M. Hasani, T. Zheng, R. Schirhagl, Nanodiamonds for in vivo applications, Small 14 (19) (2018) 1–17, https://doi.org/10.1002/smll.201703838.
[48] S.R. Hemelaar, P. de Boer, M. Chipaux, W. Zuidema, T. Hamoh, F.P. Martinez, A. Nagl, J.P. Hoogenboom, B.N.G. Giepmans, R. Schirhagl, Nanodiamonds as multi-purpose labels for microscopy, Sci. Rep. 7 (1) (2017) 720, https://doi.org/10.1038/s41598-017-00797-2.
[49] K. Terpilowski, D. Rymuszka, Surface properties of glass plates activated by air, oxygen, nitrogen and argon plasma, Glass Phys. Chem. 42 (6) (2016) 535–541, https://doi.org/10.1134/S1087659616060195.
[50] A. Morita, T. Hamoh, F.P. Perona Martinez, M. Chipaux, A. Sigaeva, C. Mignon, K. J. van der Laan, A. Hochstetter, R. Schirhagl, The fate of lipid-coated and uncoated fluorescent nanodiamonds during cell division in yeast, Nanomaterials 10 (3) (2020) 516, https://doi.org/10.3390/nano10030516.
[51] G. Jiang, S. Liu, T. Yu, R. Wu, Y. Ren, H.C. van der Mei, J. Liu, H.J. Busscher, PAMAM dendrimers with dual-conjugated vancomycin and Ag-nanoparticles do not induce bacterial resistance and kill vancomycin-resistant staphylococci, Acta Biomater. 123 (2021) 230–243, https://doi.org/10.1016/j.actbio.2021.01.032.
[52] Y.Q. Xiong, J. Willard, J.L. Kadurugamuwa, J. Yu, K.P. Francis, A.S. Bayer, Real-time in vivo bioluminescent imaging for evaluating the efficacy of antibiotics in a rat Staphylococcus aureus endocarditis model, Antimicrob. Agents Chemother. 49 (1) (2005) 380–387, https://doi.org/10.1128/AAC.49.1.380-387.2005.
[53] A.S.M. Dofferhoff, J. Buys, The influence of antibiotic-induced filament formation on the release of endotoxin from gram-negative bacteria, J. Endotoxin Res. 3 (3) (1996) 187–194, https://doi.org/10.1177/096805199600300304.
[54] T. Mokabber, H.T. Cao, N. Norouzi, P. van Rijn, Y.T. Pei, Antimicrobial electrodeposited silver-containing calcium phosphate coatings, ACS Appl. Mater. Interfaces 12 (5) (2020) 5531–5541, https://doi.org/10.1021/acsami.9b20158.
[55] H.V. Acker, J. Gielis, M. Acke, F. Cools, P. Cos, T. Coenye, The role of reactive oxygen species in antibiotic-induced cell death in burkholderia cepacia complex bacteria, PLoS One 11 (7) (2016), e0159837, https://doi.org/10.1371/journal.pone.0159837.
[56] D.I. Pattison, M.J. Davies, Actions of ultraviolet light on cellular structures, EXS 96 (2006) 131–157, https://doi.org/10.1007/3-7643-7378-4_6.
[57] A.L. Santos, V. Oliveira, I. Baptista, I. Henriques, N.C.M. Gomes, A. Almeida, A. Correia, Â. Cunha, Wavelength dependence of biological damage induced by UV radiation on bacteria, Arch. Microbiol. 195 (1) (2013) 63–74, https://doi.org/10.1007/s00203-012-0847-5.
[58] X. Qiu, G.W. Sundin, L. Wu, J. Zhou, J.M. Tiedje, Comparative analysis of differentially expressed genes in shewanella oneidensis MR-1 following exposure to UVC, UVB, and UVA radiation, J. Bacteriol. 187 (10) (2005) 3556–3564, https://doi.org/10.1128/JB.187.10.3556-3564.2005.
[59] D.-G. Yi, S. Hong, W.-K. Huh, Mitochondrial dysfunction reduces yeast replicative lifespan by elevating RAS-dependent ROS production by the ER-localized NADPH oxidase Yno1, PLoS One 13 (6) (2018), e0198619, https://doi.org/10.1371/journal.pone.0198619.
[60] J.R.A. Lancaster, Tutorial on the diffusibility and reactivity of free nitric oxide, Nitric Oxide 1 (1) (1997) 18–30, https://doi.org/10.1006/niox.1996.0112.